Mater. Res. Soc. Symp. Proc. Vol. 1204 © 2010 Materials Research Society 1204-K10-26

In-situ TEM-STM Observations of SWCNT Ropes/Tubular Transformations

F. Solá[1a], M. Lebrón-Colón[1b], P.J. Ferreira[2], L. F. Fonseca[3], M.A. Meador[1b] and C. Marín[3]
[1]National Aeronautics and Space Administration (NASA), Glenn Research Center, Structures and Materials Division, 21000 Brookpark Road, Cleveland, OH 44135, U.S.A
[a]Advanced Metallics Branch; [b]Polymers Branch
[2]Materials Science and Engineering Program, University of Texas at Austin, Austin, TX, 78712, U.S.A
[3]Institute for Functional Nanomaterials and Department of Physics of the University of Puerto Rico, Rio Piedras, PO Box 23343, San Juan, PR 00931, U.S.A.

ABSTRACT

Single-walled carbon nanotubes (SWCNTs) prepared by the HiPco process were purified using a modified gas phase purification technique. A TEM-STM holder was used to study the morphological changes of SWCNT ropes as a function of applied voltage. Kink formation, buckling behavior, tubular transformation and eventual breakdown of the system were observed. The tubular formation was attributed to a transformation from SWCNT ropes to multi-walled carbon nanotube (MWCNT) structures. It is likely mediated by the patching and tearing mechanism which is promoted primarily by the mobile vacancies generated due to current-induced heating and, to some extent, by electron irradiation.

INTRODUCTION

Since the discovery of carbon nanotubes (CNTs) by Iijima [1], CNTs have been extensively studied due to their unique electrical, mechanical and thermal properties [2]. Among the various experimental techniques used to investigate these properties, *in-situ* transmission electron microscopy (TEM) has contributed significantly to the fundamental understanding of CNT's behavior. The main reason for this is that *in-situ* TEM generally allows real-time observation and manipulation of structures at atomic scale resolution [3]. To perform *in-situ* TEM experiments several TEM holders are available [3]. One of these holders, named STM holder, has led to the: 1. Discovery of superplasticity in CNTs [4], 2.Demonstration of cap-to-cap joining of two SWCNT, which may be used as a route to reconstruct a failed nanotube during electrical device performance [5], 3.Creation of tunable nanoresonators [6], 4.Observation of vacancy migration [7], 5.Demonstration of the nanopipette behavior for metal transport [8] and 6.Systematic comparative studies of transport measurements with boron nitride nanotubes [9]. In addition, the C-K energy-loss near-edge structure [10] has been used to extract bonding information of irreversibly deformed SWCNT ropes induced by the STM tip. Results show a correlation between the reduction of π bonding (by the introduction of permanent nonhexagonal defects) and the current capacity of the tubes [11]. However, most of the TEM-STM work has focused on single nanotubes rather than ropes. In this study (using the TEM-STM holder) we present evidence of current-induced morphological modifications of purified SWCNT ropes made by the HiPco (high pressure carbon monoxide) process, which are relevant to understand the experimental limits of current density in SWCNTs connectors.

EXPERIMENTAL DETAILS

SWCNTs used in this work were prepared by the HiPco method using iron pentacarboxylic as a catalyst to induce the single sheet tubular formation. The HiPco nanotubes were purified using a modified gas-phase purification technique. The process includes refluxing the nanotubes in an aqueous solution of nitric acid followed by a series of high-temperature oxidations and repeated extractions with hydrochloric acid. The last oxidation process, done at 325 ºC for 2 h, is followed by heating the SWCNTs at 425 ºC for 1 h under wet argon. Full details about the purification technique can be found elsewhere [12]. The typical yield of purified HiPco SWCNTs by this method ranges between 30 to 35%. Analysis of the HiPco SWCNTs using inductively-coupled plasma spectroscopy revealed that the iron content of the nanotubes was reduced from 22.7 wt% to less than 0.05 wt% by the purification method.

The STM-TEM experiments were carried out in a Carl Zeiss LEO-922 TEM (equipped with an Omega filter and a tungsten (W) electron thermionic source) operated at 200 kV, using a newly fabricated Nanofactory STM holder. Typical CCD image collection time was 2s. A gold wire with a diameter ~ 0.25mm was used to attach CNTs from a powder sample by adhesion forces alone. This procedure was preferred over the use of conventional organic glues, because the latter may introduce contamination and hence can lead to additional resistance in the electrical measurements. The gold (Au) wire is then mounted in the STM holder with the use of an optical microscope. Figure 1a is a close-up photograph of the STM holder-sample area. The left arrow in figure 1a marks the Au wire position. A sharp-ended electrochemically-etched tungsten tip was connected to the six-legged hat (right arrow in figure1a), which in turn was attached to a sapphire ball that can be moved with a high level of precision using a piezoelectric scanner. Subsequently, the W tip was moved carefully (with iterative correction of the eucentric height relative to the sample) until a physical contact with a nanotube rope was made. Electrical transport measurements of the ropes were made within typical times of 200 ms and the current flow direction was from the W to the Au cable. To minimize electron beam damage, the beam was blanked unless it was required for imaging. High resolution TEM (HRTEM) images of the SWCNTs rope were taken with a LaB_6 Phillips CM-200 TEM operated at 200 kV and equipped with a Gatan imaging filter. Due to the fact that the observed transformations took place in a very short period of time (of the order of seconds) and the lack of real time image recording capabilities, a routine of voltage application (~200ms) followed by the image recording (2 sec) was applied for each selected voltage.

DISCUSSION

It is well known that during the production process, SWCNTs tend to aggregate into ropes by van der Waals forces, forming a 2D hexagonal lattice [13]. Previous studies have shown that each SWCNT within the rope has a mean diameter of 1nm and length of 1μm [14]. An HRTEM image of a typical SWCNT rope is shown in figure1b. Although the rope is curved, the image shows that the rope axis is perpendicular to the electron beam direction. The alternating black/white fringes correspond to the lattice planes of SWCNTs in the rope, with each lattice plane built from a row of tubes [15]. Figure 1c is a TEM image of a SWCNT's segment along the rope where a voltage of 1-2V was applied. It is worthwhile to mention that before the application of the voltage the observable length of the rope was ~0.5 μm, indicating that half of the rope was distributed in the Au contact surface region, and the average diameter of the CNT

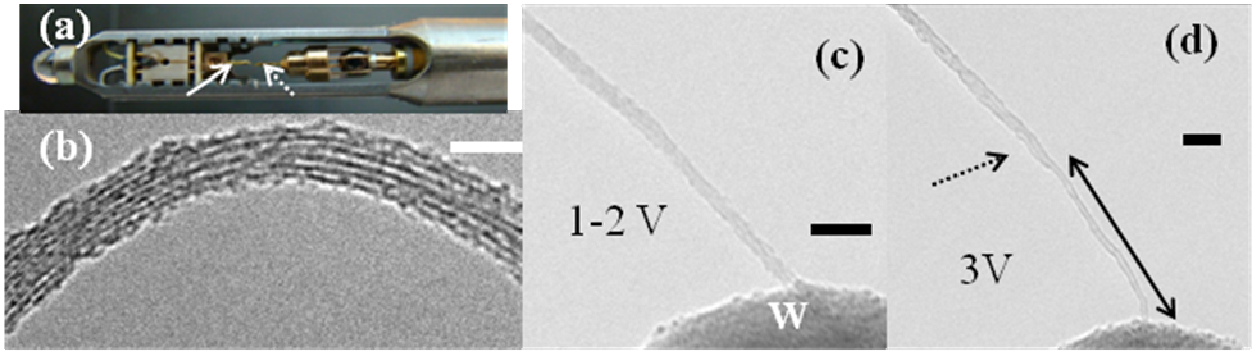

Figure 1. (a) Photograph image of the TEM-STM holder. (b) HRTEM image (scale bar is 10nm) of a SWCNT rope with a tube axis perpendicular to the e-beam. (c) and (d) are TEM images (scale bar is 20 nm) of a rope that has been exposed to a bias of 1-2V and 3V, respectively.

rope was ~5.6 nm. For 1-2V application, no evidence of morphological modifications was observed, as seen in figure 1c. When a voltage of 3V is applied to the rope (figure 1d), there are clear morphological modification, such as the appearance of kinks. In addition, buckling effects similar to those found in rail tracks caused by solar heat [16], start to appear. In our case, heat production is induced by the electrical current flowing through the rope. The diameter of the rope shrinks to ~ 3.5nm for a segment of the rope (solid arrow) of about 82 nm in length. The feature of the rope segment marked with a dotted arrow may be indicative of twisting.

When the rope is exposed to a bias of 5V, large structural modifications occur (figure 2a). This buckling behavior is indicative that a high temperature has been reached at this point, and creation and annealing of some vacancies has occurred. Protrusions with positive curvature (similar features can be observed in figure 1d), marked with arrows, may be indicative of formation of pentagonal rings from hexagonal rings by closing a divacancy during the reconstruction of the lattice, as suggested in [5] and [17]. For guidance, a schematic representation (not to scale) of figure 2a, is presented in figure 2b. For clarity, some features have been omitted. Interestingly, the buckling behavior includes a semi-circular-like geometry similar to buckling geometries predicted theoretically [18]. Relative to adjacent segments that compose the semi-circular region, angles from 148º to 167º were measured. Furthermore, the diameter near the contact region shrinks to about 2.4 nm in this 5V bias regime. Surprisingly, when a 6V bias was applied, the semicircular region disappears and a less defective tube is formed. Moreover, a clear tubular structure has been produced. Gray-value line profiles that correspond to the dotted and solid lines in figure 2c, are presented in figure 2f. The upper graph corresponds to the rope region and is noisy, while the lower graph is more consistent with a tubular structure.

Prior studies have shown that the transformation from rope to multi-wall is possible by electron irradiation [17] and conventional heat treatment [19]. It has been shown that vacancies are the dominant defects to promote the coalescence of SWCNTs. Molecular dynamics simulations revealed a patching and tearing mechanism for the coalescence and transformation from single-walled (SW) to multi-walled (MW) structures. Results indicated that this mechanism can be applicable to CNTs with different chiralities (n,m) [19]. However, this mechanism can explain either the coalescence of several SWCNTs to form a SW or the transformation to MW structure. Briefly, mobile vacancies under high temperature diffuse in the CNT towards the intertube region to create dangling bonds that form the links between neighboring SWCNTs. The links then form patches that may grow until the entire length of the CNTs is covered. Finally, the

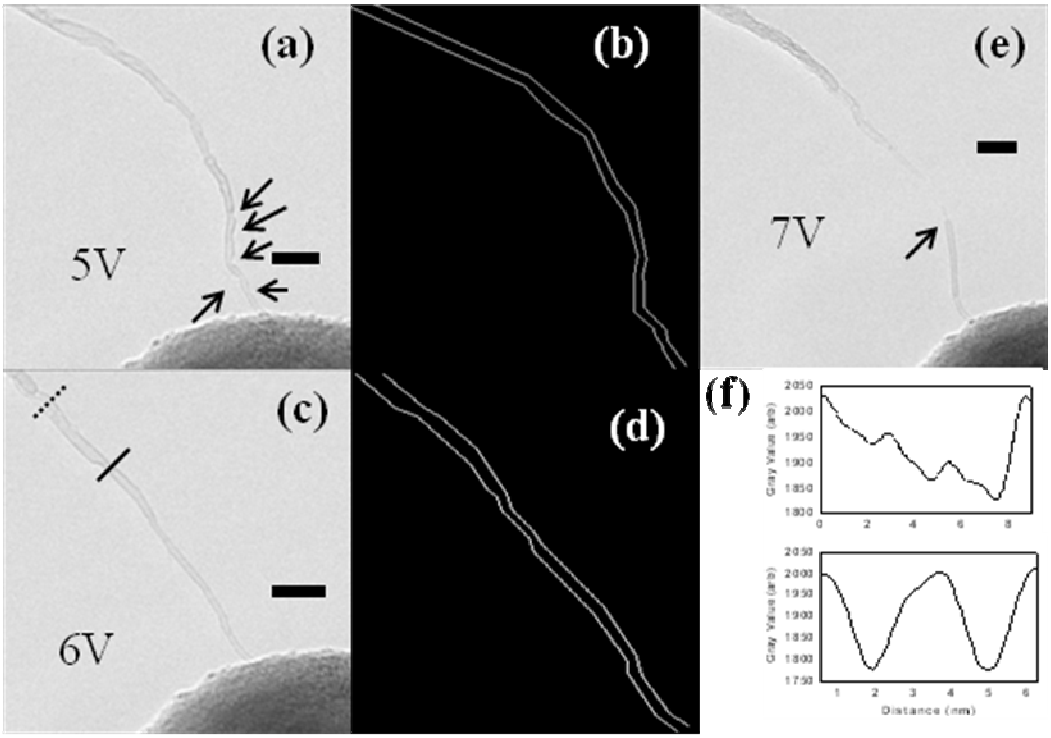

Figure 2. (a), (c) and (e) are subsequent TEM images (scale bar is 20 nm) of the same rope in fig.1 that has been submitted to a bias of 5V, 6Vand 7V respectively. (b) and (d) are schematic representations of figures (a) and (c) respectively. (f) Gray values graphs for the line profiles marked in (c).

coalescence and the SW to MW transformation process ends by tearing apart the remaining intratube bonds in the intertube region. Although the resolution limitation of the W-equipped TEM prevented us from resolving multiple walls of the tubular structure, we believe that the tubular structure in figure 2c corresponds to a MW structure because of the contrast in the walls region. Alternatively, vacancies can be created by knock–on displacements during e-beam irradiation [17]. Since a threshold energy of 86 keV has been reported for SWNT for permanent displacement [20], knock-on displacements are possible under our experimental conditions.

Knock-on displacements can be more critical for surface atoms, because the threshold energy for surface atoms may be even lower. However, as mentioned in the experimental section, we minimized beam damage irradiation by blanking the e-beam, except during imaging. Furthermore, the structural modifications were only observed when bias voltages were applied. Therefore, with these two observations, it is fair to conclude that electron beam irradiation assists in the creation of vacancies but it is not the dominating process in the transformation from SW to MW structures. A final important point regarding the cause of links between neighboring SWCNTs is the possible contribution of carboxyl and hydroxyl functional groups forming during the purification process. We believe that the contribution of functional groups is minimal for the following reasons: 1) the final annealing step in our purification process removes most of the functional groups and only small amounts remain on the surface of the CNTs and 2) previous theoretical results based on the density-functional theory predict that this would be a rare event since two close functional groups of the same type, one located in each neighboring tube, are needed for such a link [21].

It is worth to mention that the transformation we report is taking place in a time frame of the order of few seconds. The time scale for the SW to MW transformation in reference [17] was about 30 minutes, while in reference [19] was ~15 minutes. This fact strongly suggests that the production rate of defects in our work is significantly higher than in the previous mentioned works. In figure 2c one can observe that near the middle length of the tubular structure (total length is ~123 nm), the diameter is thinner. This is expected based on the Joule heating model, which predicts that the maximum temperature value is achieved in the middle region of the structure and hence can account for the significant loss of atoms in that area. At a bias of 7V, the structure's breakdown in that area as can be observed in figure 2e. The diameter of the tip-like feature, marked with the arrow in figure 2e, is about 0.5 nm, which is close to the stability limit of CNTs. Previous studies have shown that a MWCN breakdown results in the tube end forming a fullerenic cap [22]. An important observation in these experiments is that the morphological modifications start to appear near the CNT-W contact region. Similar effects of loss of material and breakdown of metal nanowires have been reported and explained in terms of electromigration and/or heating [23], whereas others have pointed out that CNTs do not suffer electromigration effects [24]. Therefore in this study, it is reasonable to assume that the observed morphological modifications should be driven by heating rather than by electromigration. Heating at the CNT-W contact region may be initiated by the presence of adsorbates or by poor physical contact [25]. Two possible areas of heating can be considered in the system under study: the nanotube itself and the CNT-W contact. The comparison between figures 1c and 1d shows that the area close to the contact is the one that initiates the transformation thus suggesting that the contact heating dominates. However, at larger voltages, the fact that the nanotube fails at the center of the modified segment, as observed in figure 2e, suggests that the Joule heating produced in the nanotube becomes important. A model in which a tubular transformation initiates at low bias voltages near the contact (which is driven by the local heating) and propagates along the tube away from the contact (reinforced by the Joule heating) of the tubular segment until failure takes place, is consistent with these observations.

CONCLUSIONS

Evidence of current-induced morphological modifications of purified SWCNT ropes made by the HiPco process, was demonstrated by *in-situ* TEM-STM. It was observed that structural modifications (buckling, kinks) appear at a bias voltage of 3V. At a bias voltage of 5V, major morphological changes appear due to the significant generation of vacancies. Protrusions with positive curvature were observed and attributed to the formation of pentagonal rings during the reconstruction of the lattice. At a bias of 6V, formation of a tubular and less defective structure was obtained. Breakdown was observed at a bias voltage of 7V. The transformations were attributed to a SW to MW structure transformation via a patching and tearing mechanism promoted mainly by mobile vacancies, which are generated by the current-induced heating, and with possible assistance from electron irradiation. The time scale for the MW structure transformation in our experiments was short in comparison with previous works where e-beam irradiation and conventional heat treatments were involved. This suggests a higher production rate of defects. Finally, our method can be used as a systematic route in the "engineering" of MWCNT-SWCNTs rope junctions, as well as to study the fundamental transport properties of such a junction with potential applications in carbon nanotube devices.

ACKNOWLEDGMENTS

This work was supported by the following grants numbers and projects: NASA NNX08BA48A, ARO W911NF-07-1-0591, Fundamental Aeronautics Program and Subsonic Fixed Wing Project. F.S. would like to thank Dr. Azlin Biaggi-Labiosa and Dr. Anita Garg both from NASA GRC, for helpful discussions.

REFERENCES

1. S. Iijima, *Nature* **354**, 56 (1991).
2. *Carbon Nanotubes: Synthesis, Structure, Properties and Applications*, ed. M.S. Dresselhaus, G. Dresselhaus and P. Avouris (Springer, Heidelberg, 2001).
3. P.J. Ferreira, K. Mitsuishi and E.A. Stach, *MRS Bulletin* **33**, 83-90 (2008).
4. J.Y. Huang, S. Chen, Z.Q. Wang, K.Kempa, Y.M. Wang, S.H. Jo, G. Chen, M.S. Dresselhaus and Z.F. Ren, *Nature* **419**, 281 (2006).
5. C. Jin, K. Suenaga and S. Iijima, *Nature Nanotechnology* **3**, 17 (2008).
6. K. Jensen, Ç. Girit, W. Mickelson and A. Zettl, *Phys. Rev. Lett*. **96**, 215503 (2006).
7. C. Jin, K. Suenaga and S. Iijima, *Nano Lett*. **8**, 1127 (2008).
8. K. Svensson, H. Olin, and E. Olsson, *Phys. Rev. Lett*. **93**, 145901-1 (2004).
9. D. Golberg, P.M.F.J. Costa, M. Mitome and Y. Bando, *Nano Res*. **1**, 166 (2008).
10. F. Solá, A. Biaggi-Labiosa, L.F. Fonseca, O. Resto, M. Lebrón-Colón and M.A. Meador, *Nanoscale Res. Lett*. **4**, 431(2009).
11. Z. Aslam, M. Abraham, A. Brown, B. Rand and R. Brydson, *J. Microscopy* **231**, 144 (2008).
12. W. Yi, A. Malkovskiy, Q. Chu, A.P. Sokolov, M. Lebrón-Colón, M.A. Meador and Y. Pang, *J. Phys. Chem.* **B112**, 12263 (2008).
13. C. Marín, M.D. Serrano, N. Yao and A.G. Ostrogorsky, *Nanotechnology* **13**, 218 (2002).
14. P. Nikolaev, M. J. Bronikowski, R. K. Bradley, F. Rohmund, D.T. Colbert, K.A. Smith and R.E. Smalley, *Chem. Phys. Lett.* **313**, 91 (1999).
15. Ph. Lambin, A. Loiseau, C. Culot and L.P. Biró, *Carbon* **40**, 1635 (2002).
16. *Wheel/Rail Interface Handbook*, ed. R. Lewis and U.Olofsson (CRC Publisher, 2009).
17. J. Li and F. Banhart, *Nano Lett*. **4**, 1143 (2004).
18. G. Cao and X. Chen, *Phys. Rev.* **B73**, 155435 (2006).
19. María J. López, A. Rubio, J. A. Alonso, S. Lefrant, K. Méténier and S. Bonnamy, *Phys. Rev. Lett*. **89**, 255501-1 (2002).
20. B.W. Smith and D.E. Luzzi, *J. Appl. Phys*. **90**, 3509 (2001).
21. A. Kis, G. Csányi, J. Salvetat, T. Lee, E. Couteau, A.J. Kulik, W. Benoit, J. Brugger and L.Forró, *Nature Mater*. **3**, 153 (2004).
22. M.A.L. Marques, H.E. Troiani, M. M. Yoshida, M. J. Yacaman, A. Rubio, *Nano Lett.* **4**, 811 (2004).
23. F.O. Hadded and C. Durkan, *Appl. Phys. Lett*. **91**, 123120 (2007).
24. M. Nihei, A. Kawabata, D. Kondo, M.Horibe, S.Sato, and Y. Awano*, Jpn. J. Appl. Phys*. **44**, 1626 (2005).
25. L. Dong, S. Youkey, J. Bush, J. Jiao, V.M. Dubin and R.V. Chebiam, *J. Appl. Phys*. **101**, 024320 (2007).